

Measurement of the response of the Russian-American Gallium
Experiment to neutrinos from a ^{51}Cr source

J.N .Abdurashitov, V .N .Gavrin, S.V .Girin, V .V .Gorbachev, T .V .Ibragimova,
A .V .Kalikhov, N .G .Khaibasov, T .V .Kodel, V .N .Komoukhov, I.N .Mimov,
A .A .Shikhin, E .P .Veretenkin, V .M .Vernul, V .E .Yants, and G .T .Zatsepin
Institute for Nuclear Research, Russian Academy of Sciences, 117312 Moscow, Russia

Yu.S.Khom yakov and A .V .Zvonarev^y
Institute of Physics and Power Engineering, Obninsk, Russia

T .J.Bowles, J.S.Nico^z, W .A .Teasdale, and D .L.Wark^x
Los Alamos National Laboratory, Los Alamos, NM 87545, USA

M .L.Cherry
Louisiana State University, Baton Rouge, LA 70803, USA

V .N .Karaulov, V .L .Levitin, V .I.Maev, P .I.Nazarenko, V .S.Shkol'nik, and N .V .Skorikov
Mangyshlak Atomic Energy Complex, Aktau, Kazakhstan

B .T .Cleveland, T .Daily, R .Davis, Jr., K .Lande, C .K .Lee, and P .W .Wilderhain
University of Pennsylvania, Philadelphia, PA 19104, USA

S.R .Elliott and J.F .Wilkerson
University of Washington, Seattle, WA 98195, USA
(21 May 2019)

^yPresent Address: Institute of Theoretical and Experimental Physics, 117259 Moscow, Russia.

^zDeceased.

^xPresent Address: National Institute of Standards and Technology, Bldg 235/A 106, Gaithersburg, MD 20899, USA.

^{*}Present Address: Department of Particle and Nuclear Physics, Oxford University, Keble Road, Oxford OX1 3RH, UK.

Abstract

The neutrino capture rate measured by the Russian-American Gallium Experiment is well below that predicted by solar models. To check the response of this experiment to low energy neutrinos, a 517 kCi source of ^{51}Cr was produced by irradiating 512.7 g of 92.4% enriched ^{50}Cr in a high flux fast neutron reactor. This source, which mainly emits monoenergetic 747 keV neutrinos, was placed at the center of a 13.1 tonne target of liquid gallium and the production rate of ^{71}Ge by the inverse beta decay reaction $^{71}\text{Ga}(\bar{\nu}_e; e^-)^{71}\text{Ge}$ was measured. The ratio of the measured rate of production of ^{71}Ge to the rate anticipated from the source activity was $0.95^{+0.11}_{-0.10}$ (stat.) $^{+0.06}_{-0.05}$ (syst.) $^{+0.035}_{-0.027}$ (theor.).

This good agreement between prediction and observation implies that the overall experimental efficiency for the solar neutrino measurements is correctly determined. Further, it establishes that there are no unknown systematic errors at the 10% level, and provides considerable evidence for the reliability of the solar neutrino measurement.

PACS codes: 26.65.+t, 95.85.Ry

I. INTRODUCTION

Gallium experiments are uniquely able to measure the principal component of the solar neutrino spectrum. This is because the low threshold of 233 keV [1] for inverse beta decay on the 40% abundant isotope ^{71}Ga is well below the endpoint energy of the neutrinos from proton-proton fusion, which are predicted by standard solar models to be about 90% of the total flux. The Russian-American Gallium Experiment (SAGE) has been measuring the capture rate of solar neutrinos with a target of gallium metal in the liquid state since January 1990. The measured capture rate [2] is 69 ± 10 (stat.) $^{+5}_7$ (syst.) SNU¹, a value that is well below solar model predictions of 137 ± 8 SNU [3] and 125 ± 5 SNU [4]. In addition, the GALLEX collaboration, which has been measuring the solar neutrino capture rate since 1991, observes a rate of $70 \pm 7 \pm 5$ SNU [5].

The other two operating solar neutrino experiments, the chlorine experiment [6] and the Kamikande experiment [7], have significantly higher energy thresholds, and thus are not able to see the neutrinos from pp fusion. When the results of these four solar neutrino experiments are considered together, a contradiction arises which cannot be accommodated by current solar models, but which can be explained if one assumes that neutrinos can transform from one species to another [8,9,10,11,12,13,14].

The gallium experiment, in common with other radiochemical solar neutrino experiments, relies on the ability to extract, purify, and count, all with well known efficiencies, a few atoms of a radioactive element that were produced by neutrino interactions inside many tons of the target material. In the case of 60 tonnes of Ga, this represents the removal of a few tens of atoms of ^{71}Ge from 5×10^{29} atoms of Ga. To measure the efficiency of extraction, about 700 g of stable Ge carrier is added to the Ga at the beginning of each exposure, but even after this addition, the separation factor of Ge from Ga is still 1 atom in 10^{11} . This impressively stringent requirement raises legitimate questions about how well the many efficiencies that are factored into the final result are known. It has been understood since the outset that a rigorous check of the entire operation of the detector (i.e., the chemical extraction efficiency, the counting efficiency, and the analysis technique) would be made if it is exposed to a known flux of low-energy neutrinos. In addition to verifying the operation of the detector, such a test also eliminates any significant concerns regarding the possibility that atoms of ^{71}Ge produced by inverse beta decay may be chemically bound to the gallium (so-called 'hot atom chemistry') in a manner that yields a different extraction efficiency than that of the natural Ge carrier. In other words, it tests a fundamental assumption in radiochemical experiments that the extraction efficiency of atoms produced by neutrino interactions is the same as that of carrier atoms.

Although a direct test with a well-characterized neutrino source lends significant credibility to the radiochemical technique, we note that numerous investigations have been undertaken during the SAGE experiment to ensure that the various efficiencies are as quoted [2]. The extraction efficiency has been determined by a variety of chemical and volumetric measurements that rely on the introduction and subsequent extraction of a known amount of the stable Ge carrier. A test was also carried out in which Ge carrier doped with a known

¹1 SNU corresponds to one neutrino capture per second in a target that contains 10^{36} atoms.

number of ^{71}Ge atoms was added to 7 tonnes of Ga. Three standard extractions were performed, and it was demonstrated that the extraction efficiencies of the carrier and ^{71}Ge follow each other very closely. Furthermore, a separate experiment was performed to test the hypothesis that atomic excitations may tie up ^{71}Ge in a chemical form that is not efficiently extracted. The radioactive isotopes ^{70}Ga and ^{72}Ga were produced in liquid gallium. These isotopes quickly beta decay to ^{70}Ge and ^{72}Ge . The excitations during beta decay should be the same as in inverse beta decay, since the driving mechanism for such excitations is the sudden change in the Coulomb charge of the nucleus. The Ge isotopes were extracted and their number measured by mass spectrometry. The results were consistent with the number expected to be produced based on the known neutron flux and capture cross section. Finally, the initial removal of the cosmogenically produced ^{68}Ge from the Ga was monitored. Before the Ga was brought underground, this nuclide was generated in the Ga as it resided on the surface exposed to cosmic rays. Initial extractions to remove this ^{68}Ge saw a reduction in the ^{68}Ge content consistent with the measured efficiencies. These numerical checks and auxiliary measurements have been a source of confidence in our methodology, yet it is clear that a test with an artificial neutrino source of known activity provides the most compelling validation of radiochemical procedures.

This article is an elaboration of work that previously appeared in Ref. [15]. The experimental changes since the previous Letter are some minor refinements in the selection of candidate ^{71}Ge events and in the treatment of systematic errors; recent cross section calculations are also included. The central experimental result given here is almost identical to what was reported earlier.

II. THE SOURCE

A. The Choice of Chromium

A number of K-capture isotopes that can be produced by neutron irradiation in a high-flux reactor, ^{51}Cr , ^{65}Zn , and ^{37}Ar , have been suggested [16,17,18,19] as sources that can be used to check the response of solar neutrino detectors. The isotope ^{51}Cr emits neutrinos with energy closest to the pp neutrinos, the solar neutrino component to which gallium is most sensitive, and thus is the best choice for the gallium experiments.

The decay of ^{51}Cr is by electron capture, $^{51}\text{Cr} + e^- \rightarrow ^{51}\text{V} + \nu_e$, with a half-life of 27.7 d. The decay scheme is illustrated in Fig. 1. There is a 90.12% branch [20] that decays directly to the ground state of ^{51}V , and a 9.88% branch which decays to the first excited state of ^{51}V , which promptly decays with the emission of a 320-keV gamma ray to the ground state. Taking into account the atomic levels to which transitions can occur, the neutrino energies are 752 keV (9%), 747 keV (81%), 432 keV (1%), and 427 keV (9%).

The intensity of the ^{51}Cr source must be high enough that the production rate in the gallium target is significantly greater than the solar neutrino capture rate. The source activity is thus required to be near to one MCi, far surpassing the activity of most sources produced at reactors. Because ^{50}Cr has only a 4.35% natural abundance, it is impossible to produce the necessary activity of ^{51}Cr by irradiation of natural Cr in any presently existing nuclear reactor. The required activity can only be attained by irradiation of enriched ^{50}Cr , as shown in Ref. [21] and additionally considered in Ref. [22]. Besides decreasing the irradiated

mass to a value that can be acceptably placed in a reactor, the use of enriched Cr reduces the self-shielding during irradiation and reduces the neutron competition from ^{53}Cr , whose capture cross section for thermal neutrons is very high.

The chromium used in our experiment was enriched to 92.4% in ^{50}Cr . The isotopic composition is given in Table I. The advantage of this high enrichment was that it yielded a source of great specific activity (more than 1 kCi/g) and small physical size, thus giving a very high neutrino capture rate (see Section V).

B. Cr Preparation

Enriched chromium was produced by the Kurchatov Institute by gas centrifugation of chromium oxyfluoride, CrO_2F_2 [23,24]. The highly corrosive CrO_2F_2 was then hydrolyzed to chromium oxide, Cr_2O_3 . To obtain an extremely compact source, the chromium oxide was then reduced to metallic chromium. This reduction was done by heating a cold-pressed mixture of chromium oxide and high purity graphite in a hydrogen atmosphere; the resulting product was melted in an Al_2O_3 crucible to remove gaseous impurities. The Cr ingots were then crushed into pieces of 1 mm to 3 mm size and the chromium was treated with hydrogen at 1200 C for 24 hours to remove residual oxygen and nitrogen.

For the reactor irradiation the metallic Cr was extruded into the form of rods, 45 mm long by 7 mm in diameter. Cr chips were placed into a molybdenum-lined steel shell under modest pressure at room temperature and the shell was electron beam welded in vacuum (10^{-6} torr). This shell with the enclosed chromium was subjected to very high pressure at 1100 C for 30 seconds and then extruded at 1000 C such that the length of the Cr was increased by a factor of 7. The steel shell was then dissolved in nitric acid and chromium rods of the desired size were produced by machining and spark cutting. Finally, the rods were recrystallized at 1000 C. The measured density (taking into account the Cr isotopic composition), grain size, and hardness of the resulting rods were very close to those of pure defectless metallic chromium. Table II gives the properties of the 50 rods that were prepared. Their microstructure was essentially identical to that of pure metallic Cr.

C. Cr Irradiation and Source Assembly

The Cr was irradiated at the BN-350 fast breeder nuclear reactor at the atomic power station in Aktau, Kazakhstan. This reactor was designed for simultaneous power and secondary nuclear fuel production. Other similar reactors are BN-600 in Russia, Phenix and Super Phenix in France, and MONJU in Japan. BN-350 has a core of highly enriched uranium without a moderator and a blanket of unenriched uranium; liquid Na is used as a coolant. This construction gives a high flux of fast neutrons [to $5 \cdot 10^{15}/(\text{cm}^2\text{s})$ at nominal power], which is advantageous for making intense sources [25]. A map of this reactor is given in Fig. 2.

The cross section for capture of fast neutrons by ^{50}Cr is less than 0.1 barn, much too low to reach the desired specific activity of ^{51}Cr . Therefore a unique irradiation assembly (called 'IA' in the following) was developed, which could be placed in the BN-350 core as a replacement fuel assembly (see Fig. 3 and Fig. 4). Most of the volume of the IA consisted

of a zirconium hydride moderator around a central stainless steel tube that contained the ^{50}Cr metal rods. This gave a high flux of low energy neutrons in the vicinity of the ^{50}Cr , and as a result, a much increased average capture cross section (4 barns). To prevent leakage of these low energy neutrons from the IA, which could increase the power release in neighboring fuel assemblies, the moderator was surrounded by absorbing elements made of europium oxide. Lastly, the presence of the IA results in a negative reactivity effect. To compensate for this the standard configuration of the reactor core was altered by replacing a few assemblies with ones of higher fuel enrichment and by installing a few additional fuel assemblies.

Calculations showed that by using two irradiation assemblies we would expect to produce a source whose activity at the end of irradiation was between 0.5 MCi to 0.8 MCi, depending on reactor power and the position in the reactor core where the IA was irradiated. The final physical characteristics of the IA were measured in a low power experiment, which was carried out in the BN-350 reactor before the full-scale irradiation. This experiment showed safe irradiation of the IA but gave less ^{51}Cr activity than anticipated. To compensate for this reduced activity it was decided to increase the reactor power near the end of irradiation. The IAs were installed on 4 September 1994 with the reactor power set at its usual level of 520 MW. Irradiation continued until 2 December, at which time the power was increased to 620 MW, so as to increase the final ^{51}Cr activity. The IAs were removed from the reactor on 18 December 1994. Using remote manipulators inside a hot cell, all 46 irradiated Cr rods were removed from the IAs and 44 of them, whose total mass before irradiation was 512.7 g, were placed into holes in a tungsten holder. This holder was then put into a stainless steel casing and the assembly was welded shut and leak checked in a helium atmosphere. This source assembly was placed in a specially constructed tungsten radiation shield with 18 mm wall thickness, which had an outer stainless steel casing of 80 mm diameter by 140 mm height. The outer stainless shell was also welded shut and leak checked. A cut-away view of the overall source assembly is shown in Fig. 5. This source was placed into a shipping cask, flown to the Mineralnye Vody airport in southern Russia, and then transported by truck to the Baksan Neutrino Observatory where the ^{51}Cr irradiations of the gallium were carried out.

D. Source Impurities

There exist a large number of chemical elements that, upon irradiation, produce long-lived gamma-emitting isotopes. The presence of these gamma emitters in the source must be strictly controlled because they increase the size of the source shield necessary for personnel protection, and thus decrease the effective neutrino path length in the gallium target, and they add heat to the source and thus confuse the calorimetric measurement of source activity which will be described below. Because of their high capture cross section for thermal neutrons, even minute quantities of some elements cannot be tolerated.

As a consequence, special care was taken in all the stages of chemical processing to minimize contamination of the Cr. To be confident that the final impurity content of the Cr rods was satisfactory, each rod was chemically analyzed before irradiation by ICP-mass spectrometry with laser ablation and by spark mass spectrometry. The concentrations of the most relevant impurities are given in Table III, together with the expected and measured

activities after irradiation. The dose rate at the side surface of the source was 1.7 Sv/h at the beginning of the first exposure (26 Dec. 1994) and only 2% of this was due to impurities (mostly ^{46}Sc). At the end of the last exposure (23 May 1995), the dose rate had decreased to 0.05 Sv/h, with an increase in the fraction due to impurities to 25%.

Figure 6 shows a gamma spectrum of the source taken shortly after the start of the first Ga irradiation. The 320-keV gamma ray from ^{51}Cr decay was attenuated by a large factor by the tungsten shield, but still was the most intense line in the spectrum. The higher energy lines of ^{46}Sc , ^{59}Fe , ^{60}Co , and ^{182}Ta had much smaller attenuations and thus produced lines, even though their activity was much lower than that of ^{51}Cr . Limits on the level of contamination activity can be inferred from this spectrum and are summarized in Table IV. The 1.5 Ci activity of ^{46}Sc was the largest single contribution and the total activity of all contaminants was estimated to be less than 2 Ci at this time.

Table III compares the values of activities expected from the pre-irradiation impurity determinations and those measured afterwards. The only significant difference was for Ta, which was because the mass-spectrometric analysis preferentially sampled the surface of the Cr rods and not the bulk material. The apparently high concentration of Ta in the Cr resulted from surface contamination by the tungsten carbide tool used to machine the rods to the desired diameter.

III. EXTRACTION SCHEDULE

The 55 tonnes of Ga that SAGE uses for solar neutrino measurements is contained in 8 chemical reactors with approximately 7 tonnes in each. Figure 7 shows the layout of the 10 reactors in the experimental area and gives their numerical identification assignments. In normal solar neutrino operation Ga is contained in reactors 2-5 and 7-10. All reactors except number 6 are equipped with the necessary mechanical equipment for the extraction process. Reactor 6 was modified for the Cr exposures by removing its stirring mechanism and replacing it with a reentrant Zr tube on its axis which extended to the reactor center. This modification increased the capacity of reactor 6 to 13 tonnes of Ga. To begin each irradiation, a specially designed remote handling system was used (Fig. 8) to place the ^{51}Cr source inside this reentrant tube at the reactor center. At the end of each irradiation, the source was moved to an adjacent calorimeter for activity measurement, and the gallium was pumped back to the two reactors where it was stored during solar neutrino runs. The ^{71}Ge was then extracted with the usual chemical procedures [26,27].

The source arrived at Mineralnye Vody on 20 Dec. 1994. Because of a delay in customs approval, it was not delivered to the laboratory in Baksan until 26 Dec. 1994. The initial installation of the source into the Ga was at 18:00 on 26 Dec. We normalize all our results to this time. Eight extractions were conducted between 2 Jan. and 24 May 1995. See Table V for a summary of the extraction dates. The lengths of the exposure periods for the first 5 measurements were chosen so each would have approximately equal statistical uncertainty. After these initial extractions, the Cr source had decayed to the point where this was no longer possible and the final 3 extractions were done at approximately monthly intervals, the same schedule as for solar neutrino extractions.

The Cr experiment used reactors 6 through 10, shown in Fig. 7. To start the first exposure Ga was pumped from reactors 9 and 10 to irradiation reactor 6 and then the ^{51}Cr source

was inserted to the center of this reactor. At the end of exposure 1 the source was moved to the calorimeter and the Ga was pumped to reactors 9 and 10 for extraction. Immediately following this extraction, the Ga was pumped to reactor 6 from reactors 9 and 10 and the source was again placed at the center of reactor 6 to begin exposure 2. Upon completion of exposure 2, the Ga was once again pumped to reactors 9 and 10. This time, however, two extractions were done - numbers 2 and 2-2. Meanwhile 13.134 tonnes of Ga from reactors 7 and 8 was pumped to reactor 6 to begin exposure 3. This pattern of exposure/extraction was repeated for a total of 8 exposures. For exposures 1, 2, 5, and 6 the Ga was extracted in reactors 9 and 10. For exposures 3, 4, 7, and 8 the Ga was extracted in reactors 7 and 8. Second extractions followed exposures 2, 4, 6, and 7.

This extraction procedure differed somewhat from that used for the solar neutrino experiment because there was the additional step of the Ga transfer from two reactors to the irradiation vessel and back. Although there is no obvious reason why this should introduce a change in extraction efficiency, a number of tests were conducted to be confident that this efficiency was not altered by the Ga transfer. Prior to the ^{51}Cr source exposure, nine solar neutrino extractions were done from one or two reactors using all steps of the above procedure including the Ga transfer. The measured production rate in these experiments was 92 SNU with a 68% confidence range from 53 SNU to 143 SNU. This capture rate was entirely consistent with that from solar neutrinos and no change was observed in the counter background.

IV . SOURCE ACTIVITY DETERMINATION

A . Source Activity from Calorimetry

The decay of ^{51}Cr deposits energy in the form of heat in its surroundings. Since all but 1 part in 10^5 of the ^{51}Cr radiation was absorbed in the source, the source activity could be determined by measuring its heat with a calorimeter. Table VI gives a summary of the energy released in ^{51}Cr decay neglecting the energy lost to neutrinos. The average energy released which can be detected as heat is 36.67 ± 0.20 keV/decay where the uncertainties have been added in quadrature.

The special calorimeter shown in Fig. 9 was built [28] to measure the heating power from the ^{51}Cr source. It consisted of two identical calorimetric transducers located side by side. The internal section of each transducer, into which the ^{51}Cr source was placed, was a copper cup 95 mm in diameter and 150 mm high, with a wall thickness of 5 mm. The copper cup was inside the air cavity of a large 68-kg copper block. A thermopile consisting of 120 chromel-alumel thermocouples connected in series was placed between the cup and the internal wall of the copper block. Thermocouple hot junctions were distributed evenly over the cup surface; the cold junctions were fixed to the internal surface of the copper block. The voltage produced by the thermopile was thus proportional to the temperature difference between the cup and its copper block. The heat produced by the source was quite large; to improve the heat exchange 8 copper plates were placed between the cup and the copper block. The power of the source warmed the cup and provided heat that was transferred to the copper block. This can be expressed as:

$$P = c \frac{dT_s}{dt} + K \Delta T; \quad (1)$$

where P is the heat power of the source (W), c is the heat capacity of the source and the cup (J/°C), T_s is the temperature of the source and cup (°C), t is the time (s), K is the heat-transfer coefficient [J/(°C s)], and ΔT is the temperature difference between the cup and the copper block (°C). The first term in Eq. (1) represents the heating of the source-cup system; the second term describes the transfer of heat to the copper block.

To understand the operation of the calorimeter, consider a typical measurement. When the source was first put into the cup, $\Delta T = 0$, so all heat from the source served only to warm the cup. Then as the temperature of the cup increased, heat began to be transferred to the copper block and the heating rate of the cup containing the source decreased. When thermal equilibrium was reached, which required approximately 6 hours, the cup-source system was at a constant temperature and all heat produced by the source was transferred to the copper block. In this condition the signal from the thermopile was constant, and the source thermal power, by Eq. (1), was determined only by the temperature difference ΔT and the heat transfer coefficient K .

The heat transfer coefficient K was determined using electroheaters made from steel or aluminum whose outside dimensions coincided exactly with the outside dimensions of the source. The heater power was varied by controlling the current to an internal Nichrome or constantan winding. Each heater was used for calibration up to its maximum power.

The calibration curve of the thermistor reading as a function of heater power in watts is shown in Fig. 10. The uncertainty associated with each measurement was approximately 2%. A fit to the calibration curve with a second-order polynomial gave the result

$$P = 0.43(14) + 0.2418(41)V + 0.000159(16)V^2; \quad (2)$$

where P is the power in watts and V is the thermistor reading in mV. The numbers in parentheses represent the uncertainties in the final digits of each parameter. With each measurement weighted by the 2% uncertainty, χ^2 for the fit was 36.9 for 35 data values.

The heat produced by the ^{51}Cr source was measured between extractions for a total of 7 measurements. The results of these measurements are shown numerically in Table VII and graphically in Fig. 11. The uncertainty in each measurement is only that propagated from the calibration curve. Each value is normalized to the activity on 26 Dec. at 18:00 taking into account the decay of the ^{51}Cr . A weighted average of these 7 power measurements gives a value on 26 Dec. at 18:00 of 112.3 ± 0.8 watts (Fig. 11). χ^2 for this average is 6.0. As a test, we performed this same fit allowing the parameter associated with the ^{51}Cr half-life to vary. The best fit half-life was determined to be 28.03 ± 0.23 days in reasonable agreement with the known value of 27.702 ± 0.004 days [20,29].

The decay of ^{51}Cr gives an average energy release of 36.67 ± 0.20 keV/decay. Using 1.6022×10^{19} (W-s)/eV and 3.7×10^{10} decays/(Ci s), this implies a conversion factor of 4.600 ± 0.025 kCi ^{51}Cr /W. The ^{51}Cr activity at the time it was first placed in the reactor containing Ga was thus 516.6 ± 3.7 kCi, where the uncertainty is entirely statistical.

Several systematic uncertainties are associated with this source activity determination. Before taking a thermocouple measurement we waited for 12 hours to be sure that the source (or electroheater) and the copper block in the calorimeter were in thermal equilibrium. It is

estimated that the uncertainty due to different stabilization times between the source and the calibration heaters can be no more than 0.6% or 3.1 kCi.

The 0.54% uncertainty in the energy released per ^{51}Cr decay leads directly to an uncertainty of 2.8 kCi in the source activity. We should note that the value we use for the energy release differs slightly from the value of 36.510 ± 0.161 keV/decay used in Ref. [30]. There are two primary differences between these calculations: First, Ref. [30] used a branching ratio to the 320-keV level of 0.0986 [31], whereas we chose to use 0.0988 [20]. Second, Ref. [30] ignored the contribution of internal bremsstrahlung, which contributes approximately 96 eV/decay to the average [32], whereas we have included it here.

The half-life of Cr is known to 0.02%. To estimate how large an uncertainty this introduced in our source activity estimate, we repeated the fit to the Cr decay curve using a value for the half-life which differed from the known value by 1 standard deviation. This changed the power determination by 0.2% or 1.0 kCi and we take that as an estimate of the related uncertainty.

Radioactive impurities in the source can also give rise to heat which would be incorrectly attributed to ^{51}Cr . The impurity content of the source was considered above in Section IID, and the contribution of each impurity to the source power is given in Table IV. The effective Cr activity from all impurities was only 100 Ci at the reference time of 18:00 on 26 Dec. 1994, which is a completely negligible 0.02% uncertainty. Because the half-life of the impurities was longer than that of Cr, the fractional size of this error increased with time. For the final calorimeter measurement on 24 April 1995, the fraction had risen to 0.14%.

Other possible contributions to the systematic uncertainty in the calorimetric determination of the source activity have been considered, such as the escape of some of the 320-keV gamma rays of ^{51}Cr from the source. All such contributions were shown to be negligible. Table V III summarizes the various components of the source activity uncertainty that were described above. Adding the statistical and systematic components in quadrature gives the final value of 516.6 ± 6.0 kCi at the reference time.

The following subsections describe other independent methods used to measure the source activity. The calorimeter technique is the most precise and we use its result; the other methods add confidence in the calorimetric determination.

B. Source Activity from Direct Counting

This section describes an independent determination of the source activity that used a Ge(Li) detector to measure the 320-keV gamma rays emitted by ^{51}Cr . Because of the high initial activity of the source, these measurements could only be carried out after the gallium exposures at the Baksan Neutrino Observatory had finished and the source had been returned to Aktau. At that time the ^{51}Cr activity had decreased by a factor of more than 1000.

The procedure for these measurements consisted of two steps: first, the relative activity of all 44 Cr rods was measured, and second, the absolute activity of a single monitor rod was determined. For the first step, two collimators were installed in the hot chamber of BN-350. A chromium rod was placed in a special transit in front of the slit of the first collimator. The transit moved in a vertical direction using a manipulator of the hot chamber and contained a motor which rotated the rod during measurement. The position of the Cr rod in relation

to the collimator slit was controlled by electronic readout of the manipulator and by visual observation. Gamma rays passed through the slit of the second collimator and were counted by a Ge(Li) detector outside the hot cell. The activity of each rod was measured at three points along its length and the angular distribution was averaged because of the rotation of the rod. This system provided the average value of the activity of all Cr rods. The uncertainty in the relative activity of one rod was 1% and was determined by statistics, background, and the stability of the measurement geometry. The uncertainty in the sum of the relative activities of all rods was added in quadrature, resulting in an uncertainty of 0.3%.

The second step was to measure the absolute activity of the monitor rod. This rod was completely dissolved in HCl acid. A small portion of this solution was diluted to prepare samples and their activity was measured. There were two sources of uncertainty in this measurement: the primary error arose from an instability of the solution and was 3%; there was also a 1% error in sample volume.

The standard deviation of a set of measurements of the count rate in the ^{51}Cr photopeak had an uncertainty of 1.2% due to statistics, background, and a dead time correction factor. The uncertainty in the efficiency of the detector was 3%. The ratio of the mass of the monitor rod to the mass of all rods in the source had a 1% uncertainty. The quadratic sum of all these uncertainties was 4.7%. The final result of this method of source activity measurement is 510 ± 24 kCi at our reference time (18:00 on 26 Dec. 1994).

C. Source Activity from Reactor Physics

The source activity can be determined, in principle, by direct neutron transport calculations using the geometry of the reactor and the irradiation assemblies. Such a calculation has many difficulties which limit its precision. The IA is not a traditional reactor assembly and traditional methods of calculation are not fully adequate for this task. Previous experience with such calculations is with thermal reactors, which contain many similar thermal cells, or with fast reactors, which have a fast neutron spectrum. In our case we have only two thermal cells (IAs) in a large fast reactor. Even Monte Carlo calculations cannot reach a statistically sound result because the Cr rods occupy such a small fraction of the total reactor volume. Additional problems in calculation arise from unmeasured neutron reaction constants and a lack of knowledge of the neutron spectrum in the thermal region.

Despite these many difficulties, a direct calculation of the source activity has been made. Our experience from previous work indicates that the accuracy of direct calculation of the neutron field in an IA with zirconium hydride is about 20%. We can, however, make the calculated values more precise by using test results. We measured the ^{50}Cr capture reaction rate in the experimental reactor in Obninsk. Although the neutron spectrum in this reactor differs from that of the BN-350 reactor, this measurement improved the reliability of the calculation of the ^{50}Cr capture reaction rate. We also performed an experiment with an IA in July 1994 before the full-scale irradiation. In this experiment we installed a small mass of ^{50}Cr in an assembly and irradiated it at low reactor power (about 5 MW). This showed that the direct calculation gave a 15% higher activity of ^{51}Cr than experiment. If we use this correction factor to scale the direct calculation, we predict the growth of ^{51}Cr activity as a function of time after the start of irradiation that is shown in Fig. 12. At our reference

time of 18:00 on 26 December 1994, the calculated activity was 560 ± 60 kCi, in agreement with the calorimeter measurement.

V. EXPECTED PRODUCTION RATE

For a neutrino source of activity A that emits isotropically, it follows from the definition of the cross section σ , that the capture rate p of neutrinos in a material around the source can be written as the product $p = ADhLi\sigma$, where $D = N_0 f_T / M$ is the atomic density of the target isotope and hLi is the average neutrino path length through the absorbing material, i.e.,

$$hLi = \frac{1}{4} \frac{\int_{\text{Absorber}} dV_A \int_{\text{Source}} \frac{dV_S}{r_{SA}^2}}{V_S} \quad (3)$$

where r_{SA} is the distance from point S in the source to point A in the absorber and the source and absorber volumes are V_S and V_A , respectively. The values and uncertainties of the constants entering D are given in Table IX.

The Ga-containing reactor in which the ^{51}Cr source was placed was nearly cylindrical, with a dished bottom. Based on accurate measurements of the reactor shape, the path length hLi was determined by Monte Carlo integration over the source and absorber volumes to be 72.6 ± 0.2 cm. The accuracy of this integration was verified by checking its predictions for geometries that could be calculated analytically and by noting that the measured Ga mass contained in the reactor volume agreed with that predicted by the integration. The sensitivity of hLi to the reactor geometry, to the position of the source in the Ga, and to the spatial distribution of the source activity were all investigated by Monte Carlo integration, and the uncertainty given above includes these effects.

The best estimate neutrino capture cross section averaged over the four neutrino lines of ^{51}Cr is given by Bahcall [33] as $58.1 \left(1.0^{+0.036}_{-0.028} \right) \times 10^{-46} \text{ cm}^2 / ({}^{71}\text{Ga atom } ^{51}\text{Cr decay})$. The stated error is a one theoretical uncertainty and arises from uncertain knowledge of the matrix elements for the two excited states in ${}^{71}\text{Ge}$ that can be reached by ^{51}Cr neutrinos and from forbidden corrections. A consideration of the contribution of excited states has also been made by Hata and Haxton [34], who recommend that the Cr source experiment itself should be used to determine the excited state contribution. Consequently, in making our uncertainty estimate for the expected production rate, we choose to explicitly separate the 3% uncertainty in the neutrino capture cross section and label it as a 'theoretical' uncertainty.

Combining the various terms that enter the expected ${}^{71}\text{Ge}$ production rate, as given in Table IX, this rate on 26 Dec. 1994 at 18:00 was $p = 14.63 \pm 0.18$ (exp.) $^{+0.53}_{-0.41}$ (theor.) atoms/d. The production rate from the source was about 3800 SNU, 50 times higher than the rate from solar neutrinos. With the cross section uncertainty neglected, the major uncertainty in the expected production rate came from the measurement of the source activity, with a very minor contribution from the error in hLi .

In the first GALLEX ^{51}Cr experiment, the expected source production rate at the beginning of the first exposure was 10.7 ${}^{71}\text{Ge}$ atoms per day and the production rate from solar neutrinos and other background sources was 0.8 /d. Even though our source had one third the intensity of this GALLEX source, our production rate was more than one-third

higher and our background rate (see Sec. V IIB) was a factor of 3 lower. This illustrates the significant advantage of using Gallium with its high atomic density as the target for a neutrino source experiment. Further, our source had very high enrichment and consequently small physical size, leading to a large value of HLi .

V I. C O U N T I N G

The number of ^{71}Ge atoms extracted from the gallium was determined by the same procedure as used for solar neutrino measurements [35]. Very briefly, the extracted Ge was synthesized into the counting gas GeH_4 , mixed with Xe, and inserted into a very low background proportional counter. All pulses from this counter were then recorded for about the next six months. The counter body was made from synthetic quartz and cathode from ultrapure Fe; the volume was about 0.75 cm^3 . To detect and suppress background, the counter was placed in the well of a large NaI detector, which was in turn contained within a massive Cu, W, and Pb passive shield. The parameters of counting are given in Table X.

The data recording system made hardware measurements of the pulse energy, ADP (a parameter inversely proportional to the pulse rise time during the first few ns), energy and time of any NaI events that occurred within -8 ms to $+8 \text{ ms}$ of the counter pulse, and event time. In addition, all the first extractions were measured in a counting system that digitized the pulse waveform for 800 ns after pulse onset. For further details concerning our counting system, see Ref. [35].

^{71}Ge decays by electron capture with an 11.4-day half life and emits Auger electrons and x rays whose sum energy is usually either 10.4 keV (the K peak) or 1.2 keV (the L peak). The radial extent of these low energy electrons in the counter is very short, producing a pulse waveform with a fast rise time. Background events, such as a minimum ionizing particle that traverses the counter, may deposit a similar amount of energy in the counter gas, but will usually have longer radial extent and hence slower rise time. Measurement of the rise time thus gives a very powerful suppression of background. For all first extractions the rise time was determined by fitting the digitized waveform to an analytical formula [36] that describes the pulse shape in terms of the radial extent of the trajectory in the counter.

The counters had a hole in the cathode near the center of the active volume with a thin section in the quartz envelope so the gas filling could be directly irradiated with the 5.9-keV x rays from ^{55}Fe . Counters were calibrated with ^{55}Fe just before the start of counting, about three days later, one week later, and then at 2 week to 3 week intervals until counting ended. At least four ^{55}Fe calibrations were made for each run during the first month of counting, while the ^{71}Ge was decaying. For all 8 first extractions the average change in the ^{55}Fe peak position during this time was 2.4%. They were also calibrated with ^{109}Cd which surrounded the Fe cathode and made 6.4 keV x rays throughout the counter volume. For these ^{109}Cd calibrations, the source was positioned so that it did not see the side hole in the cathode; the peak position was thus representative of the response of the entire counter. By comparing the predicted position of the 6.4-keV peak based on the ^{55}Fe calibration with the actual position in the ^{109}Cd calibration, a correction factor was derived that modified the energy scale from the ^{55}Fe calibration to account for any polymerization that might be present on the anode wire in the vicinity of the side hole.

After the counting of the samples from the Cr experiment was completed, in the fall of 1995, measurements of the counting efficiency were made. Two different techniques and three different isotopes were employed: ^{37}Ar to measure volume efficiency, and ^{69}Ge and ^{71}Ge to measure the L- and K-peak efficiencies [37]. The volume efficiency of all counters used for first extractions was directly measured with ^{37}Ar . The calculated counting efficiency, using the measured pressure, GeH_4 fraction, and ^{37}Ar volume efficiency, is given for each extraction in Table X. The total uncertainty in these calculated efficiencies is 3.1%.

V II. STATISTICAL ANALYSIS

A. Event Selection

Candidate ^{71}Ge events were selected in exactly the same manner as in our extractions to measure the solar neutrino flux [35]. The first step was to apply time cuts to the data that serve to suppress false ^{71}Ge events that may be produced by Rn outside the proportional counter and by Rn added to the counter during filling. In the next step, events that were in coincidence with the surrounding NaI counter were eliminated. For the first few extractions, a histogram of the 250 events that remained which occurred during the first 30 days after extraction is given in the upper panel of Fig. 13. The darkened areas are the locations of the ^{71}Ge L and K peaks as predicted from the ^{55}Fe and ^{109}Cd calibrations. For comparison, an identical spectrum of the 113 events that occurred in these extractions during an interval of equal live time at the end of counting (more than 122 days after extraction) is given in the lower panel of Fig. 13. The ^{71}Ge L and K peaks are very obvious in the spectrum at the beginning of counting, but are absent in the spectrum at the end of counting because the ^{71}Ge has decayed away. The number of counts outside the two peaks is approximately the same in both spectra because they were produced by background processes.

Windows with 98% acceptance in energy (2 FWHM width) and 95% acceptance in rise time (0-1.0 ns in the L peak and 0-18.4 ns in the K peak) were then set around the L and K peaks. All events inside these windows during the entire period of counting were then considered as candidate ^{71}Ge events.

B. The Maximum Likelihood Analysis

The time sequence of the candidate ^{71}Ge events was analyzed with a maximum likelihood method [38] to separate the ^{71}Ge 11.4-day decay from a constant rate background. The only differences between this analysis and that done for the solar neutrino runs are that one must account for the decay of the ^{51}Cr during the period of exposure, include a fixed term for solar neutrino background, and add a carryover term arising from the ^{71}Ge that was not removed because of the approximately 15% inefficiency of the preceding chemical extraction.

The likelihood function (L) for each extraction is given by Eq. (17) of Ref. [38],

$$L = e^{-(bT_L + a)} \prod_{i=1}^N (b + ae^{-\lambda t_i})^{-1} \quad (4)$$

where b is the background rate, T_L is the live time of counting, λ_{71} is the ^{71}Ge decay constant, p_i is the probability that a ^{71}Ge atom that is extracted will decay during a time that it might be counted, and t_i are the times of occurrence of the N candidate events.

The parameter a contains contributions from the 3 separate processes (Cr source neutrinos, solar neutrinos, and carryover) that are able to give ^{71}Ge in each extraction, i.e., $a = a_{\text{Cr}} + a_{\text{solar}} + a_{\text{carryover}}$. It follows from Eq. (11) and Eq. (12) of Ref. [38] that these three terms are given for extraction k by

$$a_{\text{Cr}}^k = p_{\text{Cr}} \exp[-\lambda_{51}(t_s^k - T)]^k [\exp(-\lambda_{51} t_{\text{Cr}}^k) \exp(-\lambda_{71} t_{\text{Cr}}^k)] (1 - \frac{\lambda_{51}}{\lambda_{71}}); \quad (5)$$

$$a_{\text{solar}}^k = p_{\text{solar}}^k [1 - \exp(-\lambda_{71} t_{\text{solar}}^k)]; \quad (6)$$

$$a_{\text{carryover}}^k = a_{\text{carryover}}^{k-1} \frac{\lambda_{71}^{k-1}}{\lambda_{71}^k} \exp(-\lambda_{71} t_{\text{Ga}}^k) [1 - \frac{\lambda_{71}}{\lambda_{\text{Ga}}^k}]; \quad (7)$$

Here p_{Cr} and p_{solar} are the rates of production of ^{71}Ge by the ^{51}Cr source and solar neutrinos, respectively; λ_{51} is the decay constant of ^{51}Cr ; t_s is the starting time of each source exposure; T is the source activity reference time of 18:00 on 26 Dec. 1994; t_{Cr} and t_{solar} are the times of exposure of the Ga to the ^{51}Cr source and to solar neutrinos, respectively; ϵ is the product of extraction and counting efficiencies; and $(1 - \frac{\lambda_{51}}{\lambda_{71}})$ is the inefficiency of extraction of Ge from the Ga. With these definitions, as the source decays, the production rate p_{Cr} is automatically referred to time T .

In the maximization procedure to obtain p_{Cr} for each run, the solar production rate p_{solar} was held fixed at 0.27/day, the rate corresponding to 69 SNU [2] on 13.1 tonnes of Ga. Since second extractions followed extractions 2, 4, 6, and 7, the carryover correction was only applied to extractions 2, 4, and 6. The overall production rate from the Cr source $p_{\text{Cr}}^{\text{global}}$ was obtained by maximizing the product of the likelihood functions for each run. In these maximizations the background rates in the L and K peaks for each run were free parameters.

C. The Results

The set of Tables XI, XII, and XIII gives the results of the data analysis for the L peak, K peak, and K+L peaks. The result for the global production rate in the combined fit to the 8 extractions is $16.1^{+2.5}_{-2.3}$ /day in the L peak, $12.4^{+2.0}_{-1.8}$ /day in the K peak, and $14.0^{+1.5}_{-1.5}$ /day in the K+L peaks. The uncertainties here are all statistical. Figure 14 shows the K+L combined results for the 8 exposure/extractions. In the final 3 extractions only a few counts were produced by the ^{51}Cr source, so these results for the global production rates were almost unchanged if only the first 5 extractions were used in the combined fit.

A fit permitting the ^{71}Ge half-life to vary gave 13.5 ± 2.0 days, compared with its known half-life of 11.4 days.

Our solar neutrino results in the past have been based on events selected by ADP. Table XIV gives the results of analysis of the Cr extractions using the ADP method. (Since the ADP method is not capable of effectively analyzing the L peak, only K peak results can be presented.) The result of the global fit to the 8 extractions is $11.2^{+1.8}_{-1.7}$ /day, in good

agreement with the K-peak result that used the waveform measurement of rise time to select events.

Extraction 1 had a slight counting anomaly. The waveform digitizer was inoperative for the first 2.6 days of counting and only ADP information was available. During this short time period the events selected by ADP in the K peak were used to supplement those chosen by waveform analysis and no selection of L peak events was made.

As described above, 4 of the 8 extractions were followed with a second extraction. Three of these (Cr2-2, Cr4-2, and Cr6-2) were counted in a similar way to the primary extractions, and the results are given in Table XIV (Cr2-2 is missing because the counter failed). Because of the limited number of data acquisition channels which included a digitizer, these extractions were counted in an electronic system that was only able to make the ADP measurement of pulse shape. The combined results of extractions Cr4-2 and Cr6-2 showed no ^{71}Ge production by the ^{51}Cr source, as expected.

VIII. CONSIDERATION OF SYSTEMATIC EFFECTS

A. Uncertainty in Overall Efficiency

A summary of the various contributions to the overall systematic uncertainty is given in Table XV. Most of these components are the same as for the solar neutrino extractions, so the values for the solar runs are also given in Table XV for comparison. The overall efficiency is the product of three factors: the chemical extraction efficiency, the saturation factor, and the counting efficiency. The uncertainty in each of these efficiencies will now be considered.

The major components of the uncertainty in the chemical extraction efficiency were the amount of Ge carrier added, the measured amount of Ge carrier extracted, and the amount of residual Ge carrier remaining from previous extractions. The concentration of Ge in the GaGe alloy that was added as carrier was measured by atomic absorption spectroscopy and isotope dilution spectroscopy. The resultant total uncertainty in the amount of carrier added was 2.1%. There was a 3.5% uncertainty in the measurements of the amount of Ge that was extracted; this value was larger than for the solar runs because of the smaller number of extractions performed. There were also 0.5% uncertainties in the amount of Ga and the amount of residual Ge carrier. Adding these components in quadrature yields a total uncertainty in the chemical extraction efficiency of 4.1%.

The saturation factor for the Cr source [for solar neutrinos] is defined as the factors that multiply p_{Cr}^k [p^k] on the right-hand side of Eq. (5) [Eq. (6)]. The time of exposure to the source t_{Cr} depended only on when the source was inserted and removed from the Ga-containing reactor, and was very well established, so the uncertainty in the source saturation factor was negligible. There was a minor uncertainty in the time of solar exposure because the extraction was made from 2 reactors and the mean time of extraction was used as the end time of exposure. But since the production rate from solar neutrinos was much less than from the Cr source, the uncertainty in the solar saturation factor was also negligible.

The uncertainty in the calculated counting efficiency was mentioned in Section VI. The three components are the uncertainty in volume efficiency (0.6%), in measurements to determine peak efficiency (2.5%), and in simulations used to correct for differing GeH_4 percentages

and counter pressures (1.7%), giving a combined uncertainty of 3.1%. The uncertainty in counting also includes the statistical uncertainty arising from the limited number of events in the ^{55}Fe calibrations, which typically had 1000 to 5000 events each. There were 0.1%, 0.3%, and 0.6% uncertainties in the counting efficiency due to the uncertainties in the extrapolated ^{71}Ge L- and K-peak centroid, resolution and rise time limits, respectively. Finally, there was a +2.0% uncertainty due to gain variations during the time that the ^{71}Ge was decaying. This value is one-sided because gain drifts can only shift the ^{71}Ge peak out of the event selection window. Adding these uncertainties in quadrature gave a total uncertainty in the production rate of $^{+3.7}_{-3.1}\%$ due to the uncertainty in the counting efficiency.

B. Other Systematic Uncertainties

The final uncertainty that is common to both the Cr experiment and the solar neutrino measurements arises from the inefficiency of a 3.25-hour time cut for Rn that might be added to the counter at the time it was filled. By analyzing the first 5 extractions both with and without this cut, we found that it removed a total of 22 events assigned to ^{71}Ge . Since the cut deletes all but 10% of false ^{71}Ge events, this implies that 22 false events may remain after the cut. As the total number of events assigned to ^{71}Ge in these 5 runs after the cut was 129.4, the systematic uncertainty after the cut was thus -1.7%. The value is negative since radon decays mistakenly identified as ^{71}Ge can only increase the observed signal.

Two systematic errors in Table XV are unique to the Cr-source experiment. As discussed in Section V IIB, there is an additional contribution to the measured signal from solar neutrinos and there is a carryover correction due to the incomplete removal of ^{71}Ge in the previous chemical extraction.

Although the production of ^{71}Ge in 13 tonnes of Ga by solar neutrinos is small, it is finite and a correction is necessary. We took the solar neutrino capture rate to be 69 SNU [2] and subtracted from the observed signal an amount corresponding to that production rate. The solar neutrino rate has been measured by SAGE to a precision of 12 SNU or 17%. However the solar neutrino production was only a 6.8% correction (9.8 events out of 143.7) and thus its uncertainty resulted in a small (1.2%) uncertainty in the measured ^{51}Cr production rate.

The efficiency for extracting Ge from the Ga was typically 85%. Thus a fair amount of Ge remained in the Ga after extraction. Immediately following extractions for the solar neutrino runs, a second extraction is usually carried out. Because of these second extractions and because the time between extractions is several ^{71}Ge lifetimes, the number of Ge atoms that survive to the end of the next solar run is negligible. In the Cr experiment extraction schedule, however, this was not always the case. Second extractions were conducted only after extractions 2, 4, 6, and 7 so extractions 2, 4, and 6 contain a small contribution from ^{71}Ge produced during the previous exposure. The total number of events ascribed to ^{71}Ge was 143.7 with an uncertainty of approximately 10%. The total number of estimated carryover events was 4.0 which is determined with the same 10% uncertainty. Therefore the uncertainty in the ^{51}Cr production rate due to the uncertainty in the carryover correction was 0.3%.

Combining all these uncertainties in quadrature, the overall estimate for the systematic uncertainty in the measured production rate was $^{+5.7}_{-5.6}\%$. The final measured rate was thus $p_{\text{Cr}} = 14.0^{+1.5}_{-1.5}$ (stat.) ± 0.8 (syst.) atoms of ^{71}Ge produced per day.

IX . D I S C U S S I O N

The final result can be expressed as the ratio of the measured ${}^{71}\text{Ge}$ production rate to that expected due to the source activity,

$$R = \frac{(\rho_{\text{Cr}})_{\text{measured}}}{(\rho_{\text{Cr}})_{\text{expected}}} = 0.95^{+0.11}_{-0.10} \text{ (stat.) } + 0.06^{+0.06}_{-0.05} \text{ (syst.) } + 0.035^{+0.035}_{-0.027} \text{ (theor.):} \quad (8)$$

Combining the experimental statistical and systematic uncertainties in quadrature,

$$R = 0.95 \pm 0.12 \text{ (exp.) } + 0.035^{+0.035}_{-0.027} \text{ (theor.):} \quad (9)$$

This result is consistent with 1.0 and shows that the total efficiency of the SAGE experiment to the neutrinos from ${}^{51}\text{Cr}$ is close to 100%.

Since the experimental efficiencies are known to a higher precision than can be tested with the ${}^{51}\text{Cr}$ source, this measurement does not represent a direct calibration in an absolute sense. A more exact description is that the Cr experiment is a test of the experimental procedures and has demonstrated that there is no unknown systematic uncertainty at the 10% level. Because the ${}^{51}\text{Cr}$ neutrino spectrum differs from the solar spectrum, and the total experimental efficiency for each solar neutrino measurement is known to a higher precision than the 12% uncertainty obtained with the ${}^{51}\text{Cr}$ source, the solar neutrino measurement should not be scaled by the above ratio.

The neutrino spectrum from ${}^{51}\text{Cr}$ is very similar to that of ${}^7\text{Be}$, but at slightly lower energy. Since R is equal to unity within experimental errors, we can definitively claim that SAGE responds fully to the neutrinos from ${}^7\text{Be}$. This demonstration is important because a large suppression of the ${}^7\text{Be}$ neutrino flux from the sun is one consequence of the combined analysis of the four operating solar neutrino experiments [39,40].

Our result can also be considered as a measurement of the cross section σ_0 for capture of ${}^{51}\text{Cr}$ neutrinos by ${}^{71}\text{Ga}$. Interpreted in this way, the result is $\sigma_0 = (5.55 \pm 0.69) \times 10^{-45} \text{ cm}^2 / ({}^{71}\text{Ga atom } {}^{51}\text{Cr decay})$, where the statistical and systematic errors have been combined in quadrature. Because the half life for the ${}^{71}\text{Ge}$ to ${}^{71}\text{Ga}$ decay is well known, the part of this cross section that is due to the transition to the ${}^{71}\text{Ge}$ ground state can be accurately calculated [33], and is equal to $5.52 \times 10^{-45} \text{ cm}^2$. The portion of our experimentally determined cross section that can result from transitions to the two other states in ${}^{71}\text{Ge}$ which can be excited by ${}^{51}\text{Cr}$ neutrinos (at 175 and 500 keV above the ${}^{71}\text{Ge}$ ground state) is thus no more than $(0.03 \pm 0.69) \times 10^{-45} \text{ cm}^2$.

GALLEX has completed two ${}^{51}\text{Cr}$ measurements whose combined result is $R = 0.93 \pm 0.08 \text{ (exp.) } \pm 0.03 \text{ (theor.)}$ [41]. Both SAGE and GALLEX, which employ very different chemistries, give similar results for the solar neutrino capture rate and have verified their efficiencies with neutrino source experiments. The solar neutrino capture rate measured in Ga is in striking disagreement with standard solar model predictions and there is considerable evidence that this disagreement is not an experimental artifact.

A C K N O W L E D G M E N T S

We thank E. N. Alexeyev, J. N. Bahcall, M. Baldo-Ceolin, L. B. Bezukov, S. Brice, A. E. Chudakov, G. T. Garvey, W. Haxton, P. M. Ivanov, H. A. Kurdanov, V. A. Kuzm in,

V . V . Kuzm ino v, V . A . M atveev, R . G . H . R obertson, V . A . R ubakov, L . D . R yabev, and A . N . T avkhelidze for stim ulating our interest and for fruitful discussions. W e acknow ledge the support of the Russian A cadem y of Sciences, the Institute for Nuclear R esearch of the Russian A cadem y of Sciences, the Russian M inistry of Science and Technology, the Russian Foundation of Fundam ental R esearch, the D ivision of Nuclear P hysics of the U S D epartm ent of Energy, and the U S National Science Foundation. This research was m ade possible in part by grant M 7F 000 from the International Science Foundation, grant M 7F 300 from the International Science Foundation and the Russian G overnm ent, and award num ber RP 2-159 by the U . S . C ivilian R esearch and D evelopm ent Foundation .

REFERENCES

- [1] G. Audi and A. H. Wapstra, *Nucl. Phys. A* 595, 409 (1995); A. H. Wapstra, private communication.
- [2] J. N. Abdurashitov et al., *Phys. Lett. B* 328, 234 (1994).
- [3] J. N. Bahcall, M. Pinsonneault, and G. J. Wasserburg, *Rev. Mod. Phys.* 67, 781 (1995).
- [4] S. Turk-Chieze and I. Lopes, *Astrophys. J.* 408, 347 (1993).
- [5] W. Hampel et al., *Phys. Lett. B* 388, 384 (1996).
- [6] B. T. Cleveland et al., *Astrophys. J.* (to be published).
- [7] Y. Suzuki et al., *Nucl. Phys. B* 38, 54 (1995).
- [8] J. N. Bahcall, *Phys. Lett. B* 338B, 276 (1994).
- [9] V. Berezinsky, *Comm. Nucl. Part. Phys.* 21, 249 (1994).
- [10] A. Parke, *Phys. Rev. Lett.* 74, 839 (1995).
- [11] N. Hata, S. Bludman, and P. Langacker, *Phys. Rev. D* 49, 3622 (1994).
- [12] V. Castellani et al., *Phys. Rev. D* 50, 4749 (1994).
- [13] J. N. Bahcall et al., *Nature (London)* 375, 29 (1995).
- [14] K. M. Heeger and R. G. H. Robertson, *Phys. Rev. Lett.* 77, 3720 (1996).
- [15] J. N. Abdurashitov et al., *Phys. Rev. Lett.* 77, 4708 (1996).
- [16] V. A. Kuzmin, Ph.D. thesis, Lebedev Physics Institute, Moscow, 1967, in Russian.
- [17] L. W. Alvarez, Lawrence Radiation Laboratory, Physics Notes, Memo No. 767 (1973) (unpublished).
- [18] R. S. Raghavan, in *Proceedings of the Informal Conference on Status and Future of Solar Neutrino Research*, Upton, New York, 1978, edited by G. Friedlander, Brookhaven National Laboratory Report No. 50879, vol. 2, p. 270.
- [19] W. C. Haxton, *Phys. Rev. C* 38, 2474 (1988).
- [20] *Table of Isotopes*, edited by V. S. Shirley (John Wiley and Sons, New York, 1996), 8th ed., p. 209.
- [21] V. N. Gavrin, S. N. Dan'shin, G. T. Zatsypin, and A. V. Kopylov, Preprint Inst. Nucl. Res. P-335 (1984), in Russian.
- [22] M. Cribier et al., *Nucl. Instrum. Methods Phys. Res., Sect. A* 265, 574 (1988).
- [23] A. Tikhonov, *Nucl. Instrum. Methods Phys. Res., Sect. B* 70, 1 (1992).
- [24] G. E. Popov et al., *Nucl. Instrum. Methods Phys. Res., Sect. A* 362, 532 (1995).
- [25] A. V. Zvonarev et al., *Atomic Energy* 80, 107 (1996).
- [26] V. N. Gavrin et al., in *Proceedings Inside the Sun Conference*, Versailles, France, edited by G. Berthomieu and M. Cribier (Kluwer Academic Publishers, 1989), p. 201.
- [27] V. N. Gavrin et al., in *Proceedings Sixth International Workshop on Neutrino Telescopes*, Venice, Italy, 1994, edited by Milla Baldo Ceolin, (presso la Tipografia Franchi di Piazzola), p. 199.
- [28] I. N. Belousov et al., in *Proceedings of the International School on Particles and Cosmology*, Baksan Valley, Russia, April 1991, edited by V. A. Matveev, E. N. Alexeyev, V. A. Rubakov, and I. I. Tkachev (World Scientific Publishing, Singapore), p. 59.
- [29] C. Zhou, *Nucl. Data Sheets* 63, 229 (1991).
- [30] P. Anselmann et al., *Phys. Lett. B* 342, 440 (1995).
- [31] U. Schotzig and H. Schrader, *Halbwertszeiten und Photonenemissionswahrscheinlichkeiten von häufig verwendeten Radionukliden*, PTB-Bericht PTB-Ra-16/4, Braunschweig (1993).

- [32] *Table of Radioactive Isotopes*, edited by V. S. Shirley, (John Wiley and Sons, New York, 1986).
- [33] J. N. Bahcall, *Phys. Rev. C* 56, 3391 (1997).
- [34] N. Hata and W. Haxton, *Phys. Lett. B* 353, 422 (1995).
- [35] J. N. Abdurashitov et al., in preparation.
- [36] S. R. Elliott, *Nucl. Instrum. Methods Phys. Res., Sect. A* 290, 158 (1990).
- [37] J. N. Abdurashitov, A. O. Gusev, and V. E. Yants, in *Proceedings Eighth International School on Particles and Cosmology, Baksan Valley, Russia, April 1995*, edited by E. N. Alexeyev, V. A. Matveev, K. S. Nirov, and V. A. Rubakov (World Scientific Publishing, Singapore), p. 70.
- [38] B. T. Cleveland, *Nucl. Instrum. Methods Phys. Res.* 214, 451 (1983).
- [39] S. A. Bludman, N. Hata, D. C. Kennedy, and P. G. Langacker, *Phys. Rev. D* 47, 2220 (1993).
- [40] E. Kh. Akhmedov, A. Lanza, and S. T. Petcov, *Phys. Lett. B* 348, 124 (1995).
- [41] W. Hampel et al., *Phys. Lett. B* (to be published).
- [42] *Handbook of Chemistry and Physics*, edited by D. P. Lide, (CRC Press, Boca Raton, 1993).
- [43] W. Heuer, *Z. Physik* 194, 224 (1966).
- [44] H. Koster, F. Hensel, and E. U. Franck, *Ber. Bunsen-Ges.* 74, 43 (1970).
- [45] L. A. Machlan, J. W. Gramlich, L. J. Powell, and G. M. Lambert, *J. Res. Natl. Bur. Stand.* 91, 323 (1986).
- [46] A. W. Marshall, *Ann. Math. Stat.* 29, 307 (1958).

TABLES

TABLE I. Isotopic composition of natural Cr and of the enriched Cr in the source.

Isotope	Abundance (%)	
	Natural	Enriched
50	4.35	92.4 0.5
52	83.79	7.6 0.4
53	9.50	< 0.5
54	2.36	< 0.2

TABLE II. Properties of the Cr rods prepared for irradiation.

Characteristic	Lot 1	Lot 2	Lot 3
Number of Rods	21	21	8
Total Mass of Cr (g)	245.8	244.9	93.43
Hardness (kg/mm ²)	138	134	152
Grain Size (μm)	18	24	23
Density (g/cm ³)	6.93	6.96	6.96

TABLE III. Measured impurities in the Cr rods prior to activation and the predicted resulting activities at the reference time (18:00 on 26 Dec. 1994). These are compared to the measured activities.

Impurity	Measured Content (ppm)	Nuclide	Half-life	Activity (mCi)	
				Expected	Measured
Fe	50.0	⁵⁹ Fe	44.5 d	9	24 3
W	25.0	¹⁸⁷ W	23.9 h	23	negligible
Cu	15.0	⁶⁴ Cu	12.7 h	< 0.1	negligible
Ga	5.7	⁷² Ga	14.1 h	< 0.1	negligible
Na	3.3	²⁴ Na	15.0 h	< 0.1	negligible
Zn	3.3	⁶⁵ Zn	244. d	17	negligible
Ta	3.0	¹⁸² Ta	115. d	1930	38 5
Co	1.0	⁶⁰ Co	5.3 y	81	65 15
Sc	0.9	⁴⁶ Sc	83.3 d	860	1400 100
As	0.6	⁷⁶ As	26.3 h	2	negligible
Sb	< 0.1	¹²⁴ Sb	60.2 d	< 13	negligible
La	< 0.1	¹⁴⁰ La	40.3 h	< 0.4	negligible

TABLE IV. Measured nuclide impurities in the ^{51}Cr source and their contribution to the source activity measurement at the reference time (18:00 on 26 Dec. 1994). The power estimation assumes that all the available energy is deposited in the calorimeter. A row with the data for the ^{51}Cr is included for comparison. The conversion constant 36.671 keV/decay was used in estimating the power for the Cr.

Isotope	Q Value (MeV)	Measured Activity (Ci)		Estimated Power (watts)	Equivalent ^{51}Cr Activity (kCi)
^{46}Sc	2.37	1.400	0.1	0.0200	0.092
^{60}Co	2.82	0.065	0.015	0.0011	0.005
^{182}Ta	1.81	0.038	0.005	0.0004	0.002
^{59}Fe	1.56	0.024	0.003	0.0002	0.001
Impurity total				0.0217	0.1
^{51}Cr	0.32	516600	6000	112.3000	516.6

TABLE V. Extraction schedule and related parameters. The times of exposure are given in days of year 1995.

Extraction Name	Extraction Date (1995)	Source Exposure		Source Activity (kCi)		Solar Neutrino Exposure		Mass Ga (tonnes)	Extraction Efficiency	
		Begin	End	Begin	End	Begin	End		from Ga	into GeH ₄
Cr1	2 Jan.	4.25	1.86	516.6	443.4	10.58	2.05	13.123	0.85	0.82
Cr2	9 Jan.	2.60	9.33	435.2	367.8	1.55	9.50	13.108	0.88	0.84
Cr2-2	11 Jan.	2.60	9.33	435.2	367.8	9.50	11.46	13.094	0.85	0.71
Cr3	18 Jan.	9.65	18.32	364.9	293.7	5.45	18.50	13.134	0.86	0.80
Cr4	3 Feb.	19.04	34.32	288.5	196.8	18.50	34.49	13.119	0.89	0.85
Cr4-2	5 Feb.	19.04	34.32	288.5	196.8	34.49	36.48	13.106	0.86	0.80
Cr5	1 Mar.	34.84	60.46	194.3	102.3	11.46	60.63	13.081	0.90	0.83
Cr6	24 Mar.	61.33	83.40	100.1	57.6	60.63	83.60	13.067	0.86	0.82
Cr6-2	26 Mar.	61.33	83.40	100.1	57.6	83.60	85.45	13.054	0.85	0.79
Cr7	23 Apr.	83.99	113.33	56.8	27.3	36.48	113.52	13.090	0.84	0.81
Cr7-2	26 Apr.	83.99	113.33	56.8	27.3	113.52	116.46	13.077	0.87	0.72
Cr8	24 May	118.83	143.86	23.8	12.7	116.46	144.54	13.063	0.92	0.82

TABLE VI. Summary of the input data to the power generated during the decay of ^{51}Cr . The value for the M-shell fraction is deduced from the average of the M/L ratios for the electron capture isotopes ^{37}Ar and ^{55}Fe .

Type of Radiation	Energy (keV)	Fraction of ^{51}Cr Decays		Energy Released per ^{51}Cr Decay (keV)
Gamma	320.0852 (9) [20,29]	0.0988 (5) [20]		31.624 (160)
K Capture	5.465 [42]	0.895 (5) [43]		4.891 (25)
L Capture	0.628 [42]	0.0925 (50) [43]		0.058 (2)
M Capture	0.067 [42]	0.0125 (calc)		0.001 (small)
Int. Bremsstr.	751 (endpoint)	3.8	10^{-4}	0.096 (10) [32]
Int. Bremsstr.	430 (endpoint)	1.2	10^{-4}	0.001 (small)
Total				36.671 (197)

TABLE VII. Source power measurements with the calorimeter.

Days After 18:00 on 26 Dec. 1994	Thermocouple Voltage (mV)	Deduced Power (watts)		Power on 26 Dec. 1994 (watts)	
6.62	324.8	95.7	1.9	112.9	2.2
13.90	269.9	77.2	1.5	109.3	2.2
23.08	221.2	61.6	1.2	109.8	2.2
39.08	155.36	41.8	0.8	111.1	2.2
66.21	84.46	22.0	0.4	115.1	2.3
88.17	48.88	12.6	0.3	114.5	2.3
118.17	22.20	5.9	0.1	113.0	2.3

TABLE VIII. Summary of the uncertainties associated with the source activity as deduced from the calorimetry data. In the total, the uncertainty due to contamination is taken to be the larger of the two extremes. All uncertainties are symmetric.

Origin of Uncertainty	Uncertainty	
	Percentage	Magnitude (kCi)
Statistics (112.3 ± 0.8 watts)	0.8	3.9
Calorimeter equilibration	0.6	3.1
Power to activity conversion (4.600 ± 0.025 kCi/watt)	0.54	2.8
⁵¹ Cr half-life (27.702 ± 0.004 days)	0.2	1.0
Contamination (26 Dec. 1994)	0.02	0.10
Contamination (24 April 1994)	0.14	0.72
Total uncertainty (added in quadrature)	1.2	6.0

TABLE IX. Values and uncertainties of the terms that enter the calculation of the expected production rate. All uncertainties are symmetric. See text for a discussion of why the uncertainty in the cross section is not included in the total uncertainty.

Term	Value	Uncertainty	
		Magnitude	Percentage
Atomic density $D = N_0 f_I M$			
Ga density (g Ga/cm ³) [44]	6.095	0.002	0.033
Avogadro's number N_0 (10 ²³ atoms Ga/mole)	6.0220	negligible	negligible
⁷¹ Ga isotopic abundance f_I (atoms ⁷¹ Ga/100 atoms Ga) [45]	39.8921	0.0062	0.016
Ga molecular weight M (g Ga/mole) [45]	69.72307	0.00013	0.0002
Atomic density D (10 ²² atoms ⁷¹ Ga/cm ³)	2.1001	0.0008	0.037
Path length in GaH ₂ I (cm)	72.6	0.2	0.28
Source activity at reference time A (10 ¹⁶ ⁵¹ Cr decays/s)	1.9114	0.0022	1.2
Cross section σ (10 ⁻⁴⁶ cm ² / ⁷¹ Ga atom ⁵¹ Cr decay) [33]	58.1	+ 2:1 - 1:6	+ 3:6 - 2:8
Capture rate $p = D hLi \sigma$ (⁷¹ Ge atoms produced/day)	14.63	0.18	1.2
(Uncertainties combined in quadrature, neglecting cross section)			

TABLE X. Counting parameters. is the exponentially weighted live time after all time cuts have been applied. The second extractions were not counted in an electronics system with a digitizer so L-peak analysis could not be performed. There are no entries for Cr 2-2 as the counter failed and for Cr 7-2 as the sample was not counted.

Extraction Name	Counter Filling		Counter Efficiency Before		Day Counting		Live Time of			
	G eH ₄	Pressure	Rise time or Energy Cuts		Began in 1995		Counting (Days)			
	Fraction (%)	(mm Hg)	L peak	K peak	L peak	K peak	L peak	K peak	L peak	K peak
Cr 1	6.5	690	0.335	0.356	5.82	2.90	137.8	142.1	0.618	0.734
Cr 2	8.0	685	0.326	0.344	10.42	10.35	134.5	136.7	0.753	0.767
Cr 3	7.5	650	0.329	0.338	19.41	19.34	104.0	105.6	0.792	0.804
Cr 4	8.5	665	0.329	0.341	35.39	35.32	132.3	134.8	0.824	0.837
Cr 4-2	13.5	650		0.321		37.24		126.6		0.584
Cr 5	7.5	650	0.350	0.359	61.52	61.52	119.6	122.0	0.760	0.774
Cr 6	8.7	645	0.359	0.365	84.44	84.38	120.7	123.4	0.506	0.521
Cr 6-2	13.5	695		0.350		86.21		152.0		0.841
Cr 7	7.0	645	0.329	0.337	114.49	114.29	129.8	132.4	0.775	0.784
Cr 8	7.0	700	0.324	0.347	145.41	145.41	151.8	154.9	0.729	0.747

TABLE XI. Results of analysis of L-peak events selected by pulse shape. The production rate for the individual exposures is referred to the starting time of each exposure. The production rate for the combined result is referred to the time of the start of the first exposure. The second extractions were not counted in an electronics system with a digitizer so event selection based on pulse shape could not be made. The parameter $N w^2$ measures the goodness of fit of the sequence of event times [46]. The probability was inferred from $N w^2$ by simulation.

Extraction Name	Number of Candidate Events	Number Fit to ⁷¹ Ge	Number of Events Assigned to			⁷¹ Ge Production Rate by ⁵¹ Cr Source (atom s/day)	$N w^2$	Probability (Percent)
			⁵¹ Cr Source Production	Solar Production	Carryover			
Cr 1	23	20.9	22.5	0.4	0	28.5 ^{+6:6 6:8 6:0}	0.173	24
Cr 2	22	11.9	10.4	0.3	1.1	10.8 ^{+2:4 2:9}	0.036	81
Cr 3	22	11.9	11.4	0.5	0	10.0 ^{+4:4 3:5}	0.062	43
Cr 4	24	15.1	13.8	0.6	0.7	8.0 ^{+3:8 1:8}	0.082	37
Cr 5	20	8.8	7.9	0.9	0	4.3 ^{+2:8 1:7}	0.079	31
Cr 6	34	0.6	0.0	0.5	0.2	0.0 ^{+3:3 0:0}	0.045	82
Cr 7	14	2.9	2.1	0.8	0	1.2 ^{+2:0 0:7}	0.118	23
Cr 8	11	2.8	2.2	0.7	0	1.4 ^{+2:0 1:1}	0.067	50
Combined	170	78.2	71.6	4.7	1.9	16.1 ^{+2:5 2:3}	0.104	25

TABLE X II. Results of analysis of K -peak events selected by pulse shape. See caption for Table X I for further explanation.

Extraction Name	Number of Candidate Events	Number Fit to ^{71}Ge	Number of Events Assigned to			^{71}Ge Production Rate by ^{51}Cr Source		Probability (Percent)
			^{51}Cr Source Production	Solar Production	Carryover	(atom s/day)	$N w^2$	
Cr1	20	16.4	15.9	0.5	0	$17.2^{+5.1}_{-4.7}$	0.035	90
Cr2	18	12.2	10.6	0.4	1.2	$10.2^{+5.4}_{-2.9}$	0.319	3
Cr3	18	13.2	12.7	0.5	0	$10.5^{+3.7}_{-2.8}$	0.515	1
Cr4	12	10.4	9.1	0.6	0.7	$5.0^{+2.5}_{-1.4}$	0.060	69
Cr5	15	7.9	6.9	0.9	0	$3.6^{+2.3}_{-1.2}$	0.034	84
Cr6	8	2.8	2.1	0.5	0.2	$1.6^{+2.3}_{-1.0}$	0.041	79
Cr7	12	1.0	0.1	0.9	0	$0.1^{+1.7}_{-0.1}$	0.071	60
Cr8	10	2.0	1.2	0.7	0	$0.7^{+1.6}_{-0.5}$	0.064	59
Combined	113	67.5	60.3	5.1	2.1	$12.4^{+2.0}_{-1.8}$	0.042	87

TABLE X III. Results of combined analysis of L- and K -peak events selected by pulse shape. See caption for Table X I for further explanation.

Extraction Name	Number of Candidate Events	Number Fit to ^{71}Ge	Number of Events Assigned to			^{71}Ge Production Rate by ^{51}Cr Source		Probability (Percent)
			^{51}Cr Source Production	Solar Production	Carryover	(atom s/day)	$N w^2$	
Cr1	43	36.9	36.0	0.9	0	$22.0^{+4.1}_{-3.8}$	0.121	35
Cr2	40	24.0	21.1	0.7	2.3	$10.5^{+3.2}_{-2.9}$	0.202	3
Cr3	40	25.2	24.2	1.0	0	$10.3^{+2.6}_{-2.3}$	0.120	15
Cr4	36	25.2	22.5	1.3	1.4	$6.4^{+1.7}_{-1.5}$	0.061	61
Cr5	35	16.4	14.6	1.8	0	$3.9^{+1.5}_{-1.3}$	0.034	84
Cr6	42	4.1	2.8	0.9	0.3	$1.2^{+1.5}_{-1.0}$	0.046	79
Cr7	26	3.9	2.2	1.7	0	$0.6^{+1.0}_{-0.6}$	0.081	43
Cr8	21	4.5	3.1	1.4	0	$0.9^{+1.1}_{-0.8}$	0.034	89
Combined	283	143.7	130.0	9.8	4.0	$14.0^{+1.5}_{-1.5}$	0.068	50

TABLE X IV . Results of analysis of K -peak events selected by ADP . The second extraction results were not used in the combined fit.

Extraction Name	Number of Candidate Events	Number Fit to ^{71}Ge	Number of Events Assigned to			^{71}Ge Production Rate by ^{51}Cr Source		Probability (Percent)
			^{51}Cr Source Production	Solar Production	Carryover	(atom s/day)	$N w^2$	
Cr1	16	16.0	15.5	0.5	0	$15.3^{+4.0}_{-4.0}$	0.038	94
Cr2	15	10.8	9.3	0.4	1.2	$9.2^{+5.0}_{-2.6}$	0.235	6
Cr3	16	12.9	12.4	0.5	0	$10.4^{+3.7}_{-2.8}$	0.466	2
Cr4	9	9.0	7.7	0.6	0.7	$4.3^{+2.4}_{-1.0}$	0.055	84
Cr4-2	7	0.2	0.1	0.1	0	$0.1^{+2.0}_{-0.1}$	0.219	12
Cr5	13	5.6	4.7	0.9	0	$2.5^{+2.1}_{-1.0}$	0.027	93
Cr6	6	1.8	1.2	0.5	0.2	$0.9^{+2.0}_{-0.8}$	0.034	91
Cr6-2	5	0.1	0.0	0.1	0	$0^{+1.0}_{-0.0}$	0.086	50
Cr7	8	1.9	1.0	0.9	0	$0.6^{+1.6}_{-0.4}$	0.038	85
Cr8	11	1.8	1.1	0.7	0	$0.6^{+1.6}_{-0.5}$	0.062	60
Combined	94	61.7	54.7	5.0	2.0	$11.2^{+1.8}_{-1.7}$	0.039	89

TABLE XV. Summary of the contributions to the systematic uncertainty in the measured neutrino capture rate. Unless otherwise stated, all uncertainties are symmetric. The total is taken to be the quadratic sum of the individual contributions. For comparison, many of the systematics for the solar neutrino extractions are also provided. (Some of the solar values depend critically on the particular data set considered and are thus missing.) The statistical uncertainty in the result of the Cr experiment is $^{+10.6}_{-9.9} \%$.

Origin of Uncertainty	Uncertainty in Percent	
	for Solar Runs	for Cr Runs
Chemical Extraction Efficiency		
Mass of Added Ge Carrier	2.1	2.1
Amount of Ge Extracted	2.5	3.5
Carrier Carryover	0.5	0.5
Mass of Gallium	0.5	0.5
Chemical Extraction Subtotal	3.3	4.1
Saturation Factor		
Exposure Time	0.14	0
Lead Time	0.8	0
Saturation Factor Subtotal	0.8	0
Counting Efficiency		
Calculated Efficiency		
Volume Efficiency	0.5	0.5
Peak Efficiency	2.5	2.5
Simulations to Correct for Counter Filling	1.7	1.7
Calibration Statistics		
Centroid	0.1	0.1
Resolution	0.3	0.3
Rise time Cut	0.6	0.6
Gain Variations		+ 2.0
Rise time Window Offset		0
Counting Efficiency Subtotal	+ 4.4, 3.2	+ 3.7, 3.1
Residual Radon after Time Cuts		1.7
Solar Neutrino Background	0	1.2
⁷¹ Ge Carryover	0	0.3
Total Systematic Uncertainty		+ 5.7, 5.6

FIGURES

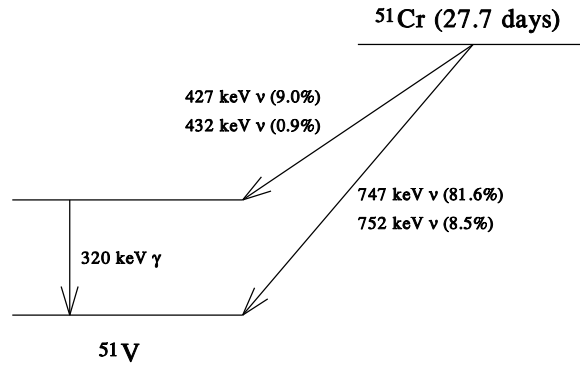


FIG . 1. Decay scheme of ^{51}Cr to ^{51}V through electron capture.

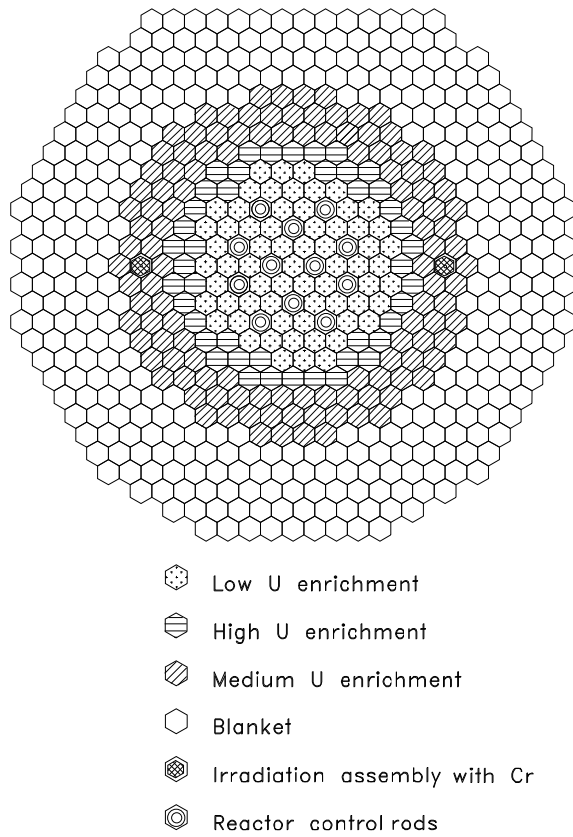


FIG . 2. Map of cells of reactor BN-350.

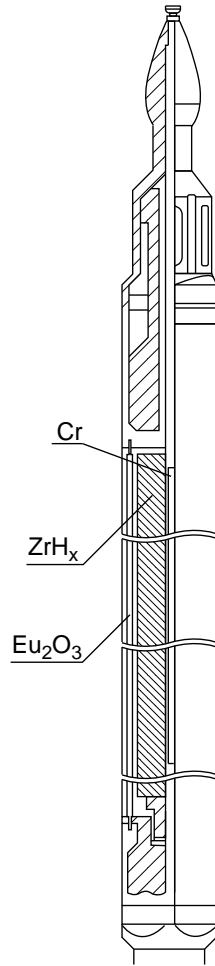


FIG .3. Irradiation assembly (IA).

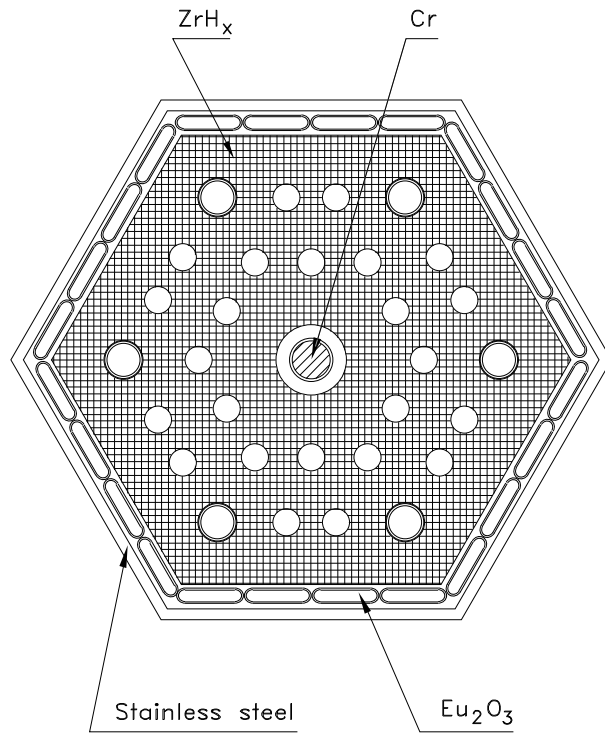


FIG . 4. Cross section of irradiation assembly (IA). The unshaded circles are cooling channels for liquid Na.

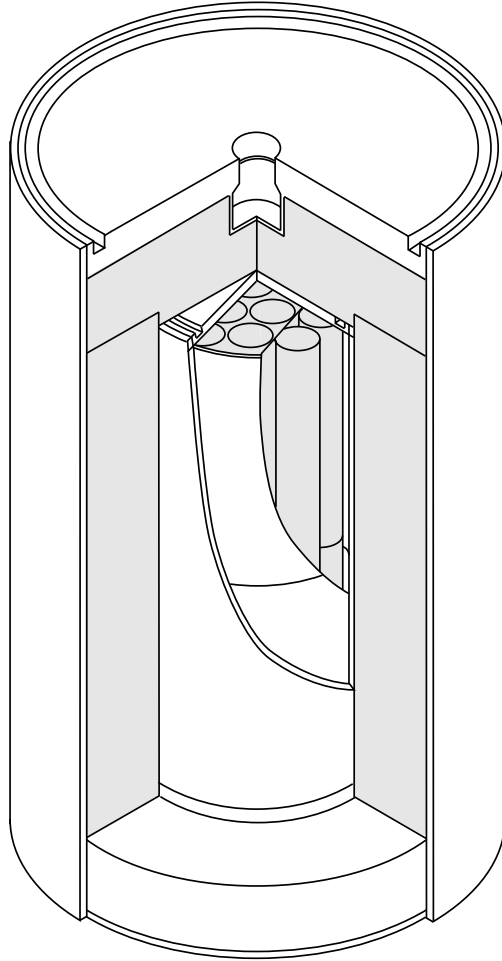


FIG . 5. Cut-away drawing of the source. The Cr rods were placed within the inner cylinders.

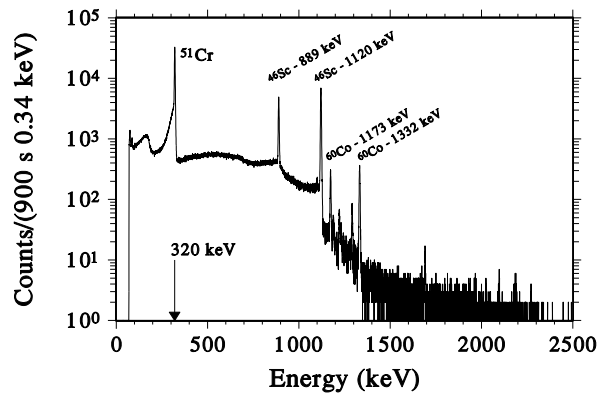


FIG . 6. Unshielded Ge detector spectrum of the gamma rays emitted by the Cr source taken on 7 January 1995 at 10:40. Gamma lines are labeled by the isotope of origin. Other contaminants whose lines are not labeled include ⁵⁹Fe, ¹⁸²Ta and ¹²⁴Sb.

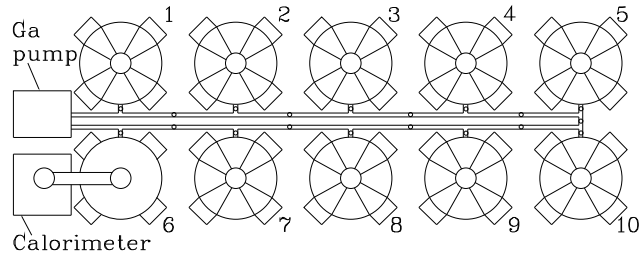


FIG . 7. Plan view of the laboratory showing the ten chemical reactors, irradiation reactor 6 with the adjacent calorimeter, and the Ga pump for transferring Ga between reactors.

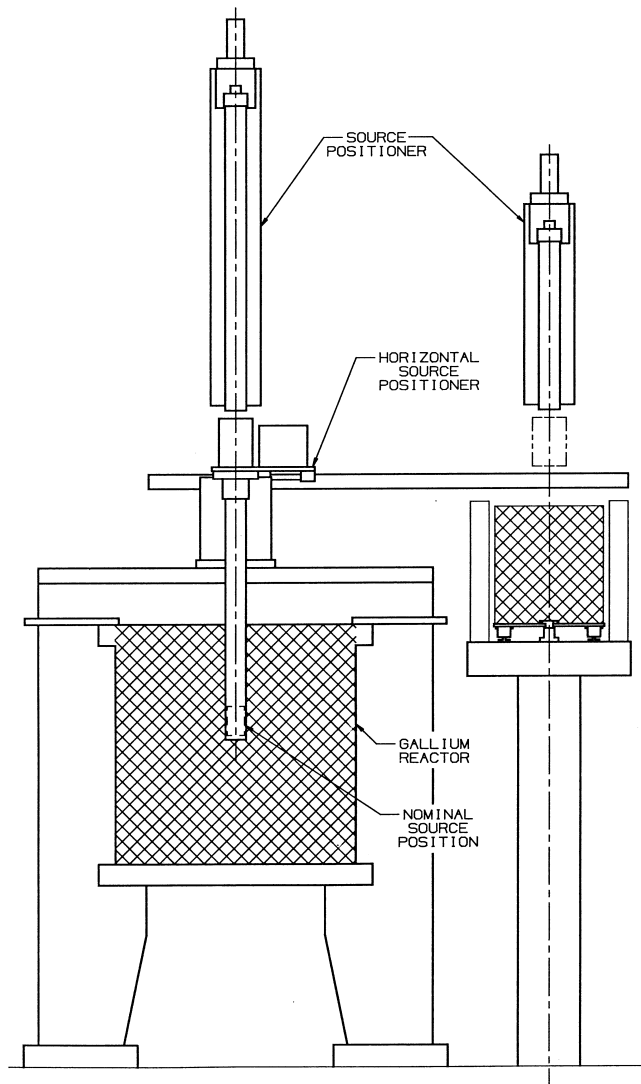


FIG . 8. Schematic drawing of the remote handling system which moved the ^{51}Cr source from the gallium-containing reactor to the adjacent calorimeter.

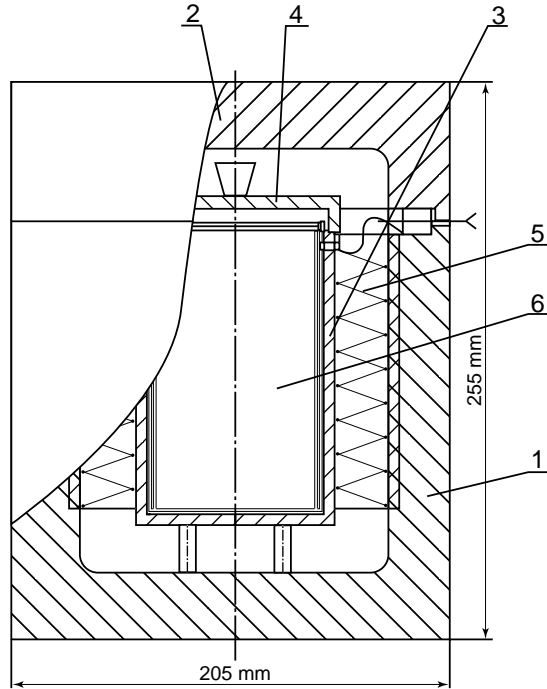


FIG .9. Schem atic drawing of the calorim eter. Individual parts are (1) copper block, (2) lid of copper block, (3) copper cup, (4) lid of copper cup, (5) them opile, and (6) source or electroheater.

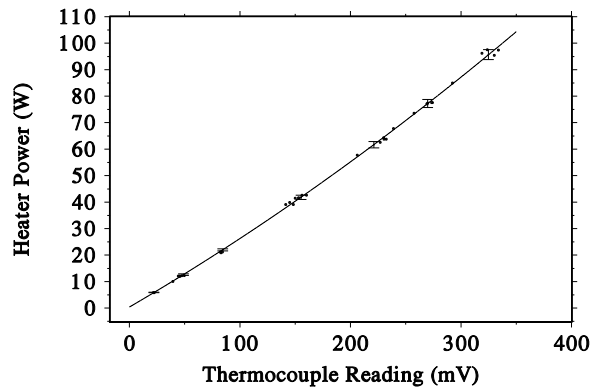


FIG .10. Calibration curve of the calorim eter. The them ocouple readings and the inferred power for the 7 m easurem ents of the C r source are also indicated.

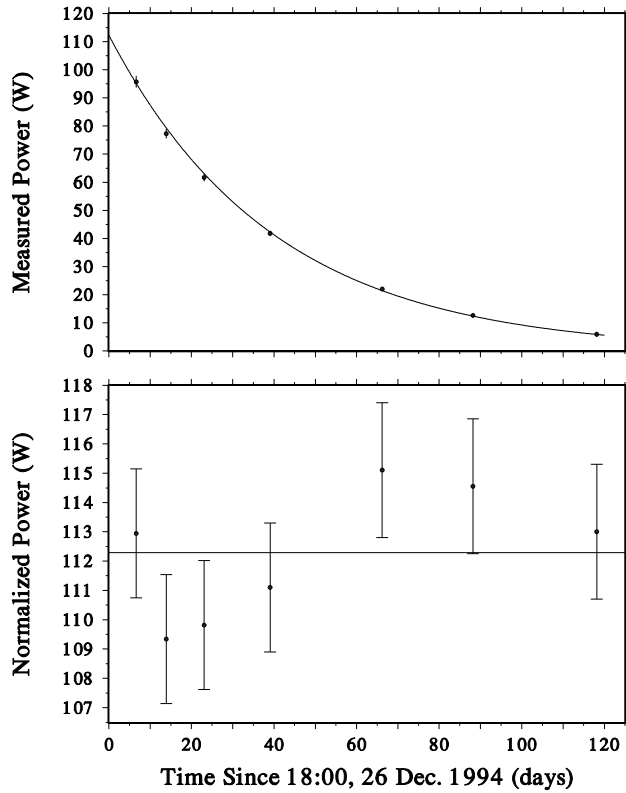


FIG .11. The 7 individual source activity measurements. The line is a weighted fit to the data points with an exponential function whose half-life is that of ^{51}Cr . In the lower panel the power is normalized to 18:00 on 26 December 1994.

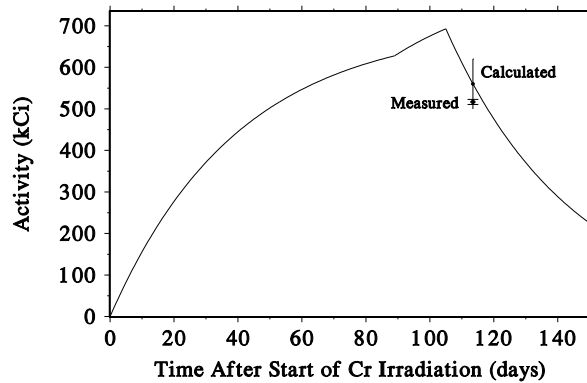


FIG .12. Time dependence of the ^{51}Cr activity. The solid curve shows the results of a direct calculation based on reactor physics that is scaled by test measurements at low reactor power. The typical error of calculation is indicated at the time when the source was first installed in the Ga. The actual source activity, as measured with the calorimeter, is also shown at this same time.

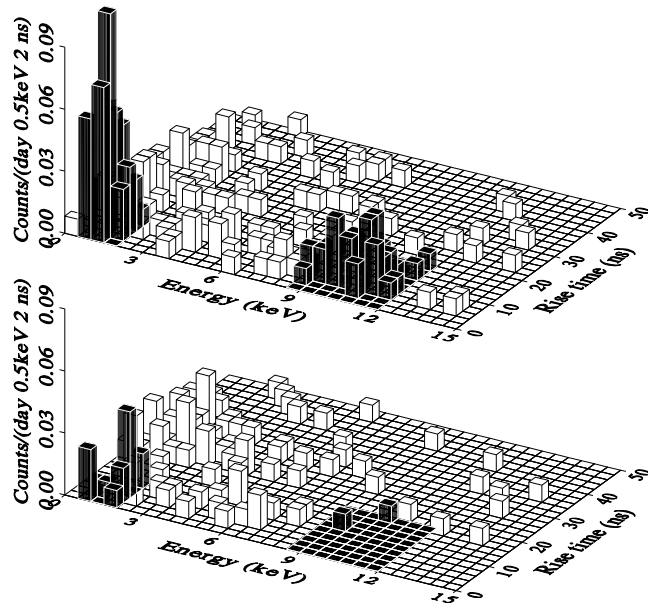


FIG. 13. Upper panel shows the energy-rise time histogram of all events observed during the first 30 days after extraction for the first 5 Cr exposure measurements. The live time is 120.1 days. The expected location of the ^{71}Ge L and K peaks is shown darkened. Lower panel shows the same histogram for all events that occurred during an equal live time interval at the end of counting.

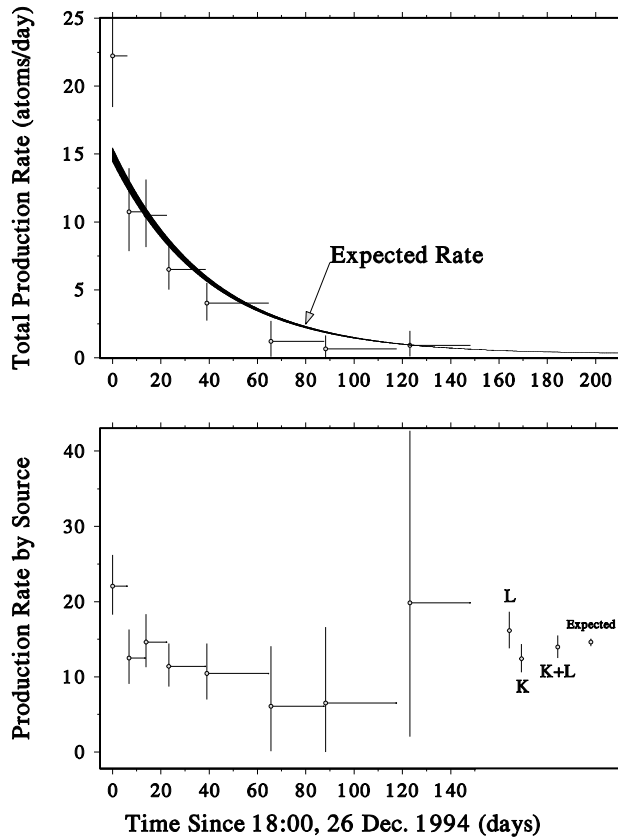


FIG . 14. The eight ^{71}Ge production rate measurements. The horizontal lines indicate the beginning and ending of each exposure with the vertical lines showing the measured production rate and its error. The upper panel shows the total ^{71}Ge production rate from the source and from solar neutrinos. The expected rate calculated from the 517 kCi source activity and the cross section of Bahcall [33] is shown darkened. The lower panel shows only the production rate from the ^{51}Cr source, where each rate has been normalized to the time of the start of the first exposure. The combined results of all measurements are shown at the right, with the L-peak, K-peak, and L-plus K-peak results shown separately. The expected production rate and its uncertainty are shown at the extreme right.